Available online at www.sciencedirect.com
SCIENCE DIRECT
C. R. Mecanique 333 (2005) 265–272
COMPTES RENDUS MECANIQUE
http://france.elsevier.com/direct/CRAS2B/

Laminar junction flow at low Reynolds number: influence of the upstream region on the comparison between experiments and calculations

Sébastien Rouvreau [a], Laurent David [b,*], Damien Calluaud [b], Pierre Joulain [a]

[a] *Laboratoire de combustion et de détonique, UPR CNRS 9028 / ENSMA, 1, avenue Clément-Ader, BP 40109, 86961 Futuroscope cedex, France*
[b] *Laboratoire d'études aérodynamiques, UMR CNRS 6609/université de Poitiers, boulevard Marie et Pierre Curie, téléport 2, BP 30179, 86960 Futuroscope cedex, France*

Received 6 April 2004; accepted after revision 24 November 2004

Available online 7 January 2005

Presented by Sébastien Candel

Abstract

The laminar flow around a square block mounted at a short distance form the leading edge of a flat plate is investigated both experimentally and numerically. The Reynolds number, based on the obstacle width, is 1000. A detailed analysis of the junction flow shows how pressure and velocity can be influenced by the proximity between the obstacle and the leading edge of the plate. Calculations with the obstacle in the vicinity of the inlet boundary are in poor agreement with experiments. A change in the computational domain geometry in the upstream side of the plate is introduced and leads to a significant improvement of the description of the vortical structure formed upstream of the obstacle. The slight discrepancies remaining between calculations and experiments have little influence on the dynamics of the wake flow description and particularly on the frequency of vortex shedding. ***To cite this article: S. Rouvreau et al., C. R. Mecanique 333 (2005).***

Résumé

Écoulement de jonction en régime laminaire à faible nombre de Reynolds : Influence de la région amont sur la comparaison calcul-expérience. Une étude expérimentale et numérique est menée sur un écoulement laminaire à $Re = 1000$ autour d'un obstacle de base carrée placé au voisinage du bord d'attaque d'une plaque plane. Une étude détaillée montre l'influence que peut avoir cette proximité entre l'obstacle et le bord d'attaque de la plaque sur le champ de pression et de vitesse. Des simulations avec une limite amont du domaine de calcul proche de l'obstacle donnent des résultats relativement différents des mesures. L'introduction d'une modification de la géométrie du domaine de calcul dans la région amont de la plaque permet une amélioration notable de la description de la structure tourbillonnaire formée autour de l'obstacle. Néanmoins, de légères

* Corresponding author.
E-mail address: laurent.david@univ-poitiers.fr (L. David).

1631-0721/$ – see front matter
doi:10.1016/j.crme.2004.11.010

différences sont encore présentes entre calcul et expérience. Leurs influences sur la dynamique de l'écoulement de sillage sont faibles, notamment pour ce qui concerne la fréquence de lâchage tourbillonnaire. ***Pour citer cet article : S. Rouvreau et al., C. R. Mecanique 333 (2005).***

Keywords: Computational fluid mechanics; Horseshoe vortex; Direct Numerical Simulation 3D; Particle Image Velocimetry; Topology

Mots-clés : Mécanique des fluides numérique ; Tourbillon en fer à cheval ; Simulation Numérique Directe Tridimensionnelle ; Vélocimétrie par Imagerie de Particules ; Topologie

1. Introduction

Flows around three-dimensional obstacles are complex and usually characterized by large unsteady rotational structures, by regular vortex shedding and by a strongly three-dimensional topology. Past investigations of these flows have focussed on their physical structures and on the identification of the parameters (upstream flow regime, shape factor of the obstacle, experimental conditions) which control the topology and the dynamics of the flow. The Reynolds number, the boundary layer thickness and nature (Hunt et al. [1], Castro and Robins [2]), dimensions and position of the obstacle (Chou and Chao [3]) and the blockage ratio prove to have a major influence on the nature of the flow. In the case of a finite-width obstacle on a flat plate, a junction flow is established in the upstream region of the obstacle due to an inversion of the pressure gradient in the boundary layer. This leads to the formation of a 3D rotational structure composed of multiple vortices known as the horseshoe vortex. For low Reynolds numbers and thin boundary layer flows, this stationary structure is a combination of 2 to 4 vortices (Baker [4]) and has a strong influence extending far upstream on the external flow.

Comparisons between experiments and calculations concerning this problem are not numerous. A few experimental (Martunizzi and Tropea [1,5]) and numerical (Rodi et al. [6]) investigations through LES calculations concerning flows around square-shaped geometries (2D and 3D geometries) mounted on flat plates for high Reynolds number, relevant for flows around buildings, have been carried out during the past few years. Nevertheless, a good agreement between experiments and calculations has not yet been reached. Comparison for the flow around a square cylinder mounted near the leading edge of a flat plate where the leading edge of the obstacle is in the vicinity of the inlet boundary are in rather poor agreement, particularly concerning the frequency of vortex release in the wake [7].

A flow around a square block mounted at a short distance of the leading edge of a flat plate and for a Reynolds number equal to 1000 (based on the velocity of the external flow and the obstacle width) is investigated both experimentally and numerically with a particular focus on the influence of the obstacle on the upstream flow. A detailed analysis of the junction flow shows how pressure and velocity can be influenced by the proximity between the leading edge of the plate and the obstacle. A change in the geometry of the calculation domain is introduced to get an improved description of the upstream vortical structure which is believed to rule the entire topology and dynamics of the flow.

2. Experimental approach

The experimental set-up is a 160 mm × 160 mm closed-loop water channel operating at velocities ranging from 1 to 5 cm/s. The obstacle is 60 mm × 60 mm and its height H is 18 mm. It is mounted on a flat plate placed at a distance of 130 mm from the upper wall of the channel and positioned at 40 mm from its leading edge. The Reynolds number of the flow ($Re = 1000$) is based on the velocity of the uniform flow, 1.8 cm/s, and the width D of the obstacle. The flow is seeded with solid particles (hollow glass particles) of diameter 15 μm. Lighting is provided by a continuous Argon laser, an optical shutter, an optic fibre and lenses. Flow images are recorded by

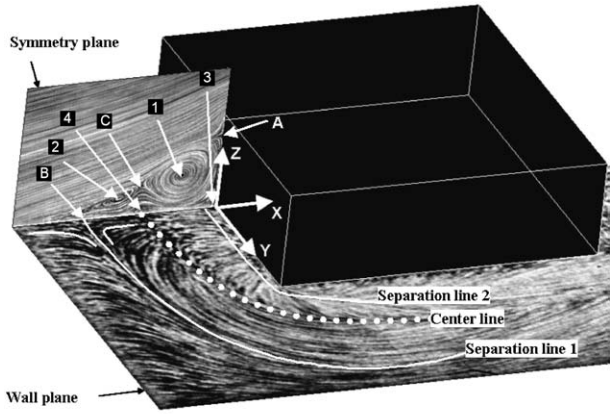

Fig. 1. Particle visualization of the flow in the symmetry plane ($Y = 0$) and the wall plane ($Z = 0$).

Fig. 1. Visualisations par particules de l'écoulement dans le plan de symétrie $Y = 0$ et sur le plan en proche paroi ($Z = 0$).

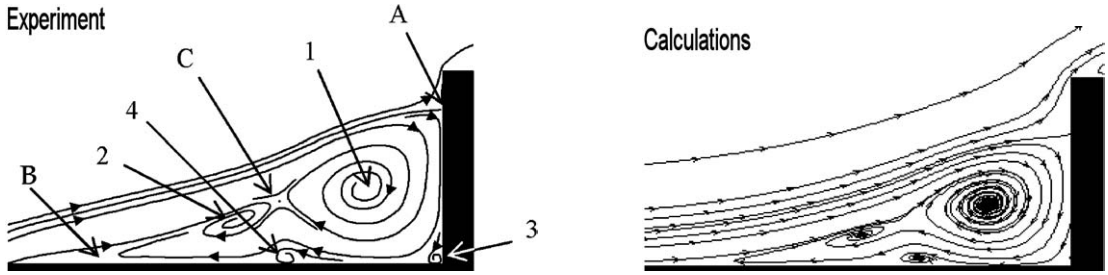

Fig. 2. (a) Singular points of the upstream vortical structure for section $Y = 0$. (b) Streamlines from the calculation for the same section.

Fig. 2. (a) Points singuliers de la structure tourbillonnaire amont pour la section $Y = 0$. (b) Lignes de courant obtenues par le calcul pour la même section.

a Nikon F4S camera or a 768 × 484 pixels CCD camera. Velocity fields are obtained through a Particle Image Velocimetry method using the Dantec software Flowmap. The double frames are processed using adaptive cross correlation via FFT on 32 × 32 pixels final size windows with an overlap of 50%. At the last step, two iterations are carried out in order to center the correlation peaks in the analysis windows and therefore improve the sub-pixel approximation, with a bidimensional spatial resolution of $1.5 \times 1.5\ \text{mm}^2$. Averaged velocity fields are calculated from 1000 instantaneous fields which imply minimum experience duration of 100 seconds beyond establishment of the flow.

Visualizations and velocity fields show a junction flow generated by the main stream hitting the upstream face of the obstacle (Fig. 1). An inversion of the pressure gradient takes place inside the boundary layer and leads to a 3D separation. This creates a strongly three-dimensional vortex flow composed of complex structures organised around a horseshoe vortex (Calluaud [8]). Position of various singular points in the symmetry plane of the vertical system have been obtained from particle streak visualizations and are given in Table 1. The stream which hits the upstream face of the obstacle, splits into two distinct parts separated by stagnation point A (Fig. 2(a)).

Below this stagnation point, fluid enters the horseshoe vortical structure composed of a four vortices, as predicted by the classification proposed by Baker [4]. The steadiness of these structures has been checked by using instantaneous velocity fields and calculated statistical properties. The flow field features two primary (1 and 2) and two secondary vortices (3 and 4). Inside this system in the vicinity of the plate, fluid flows in the upstream

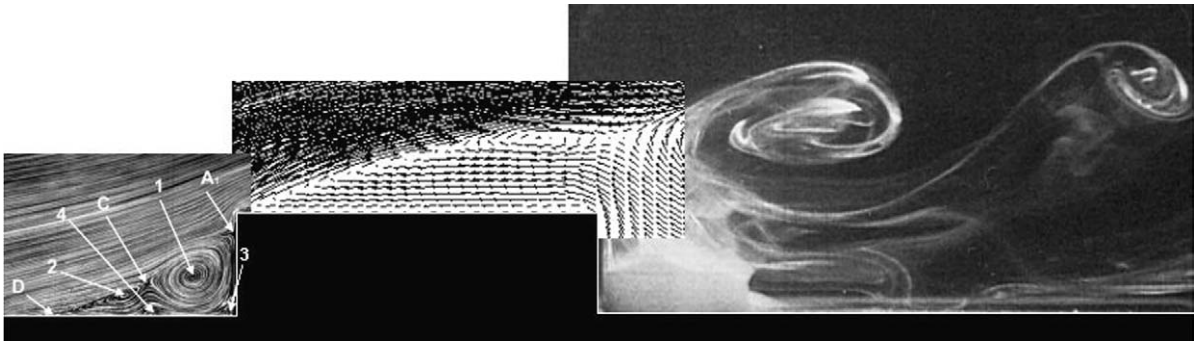

Fig. 3. Composite flow visualizations in the symmetry plane (visualization by solid particles on the upstream side of the obstacle, velocity field obtained by P.I.V., visualization by dye-emission downstream of the obstacle).

Fig. 3. Visualisations de l'écoulement dans le plan de symétrie (visualisation par particules solides sur la partie amont de l'obstacle, champ de vitesse obtenu par PIV, visualisation par émission électrochimique derrière l'obstacle).

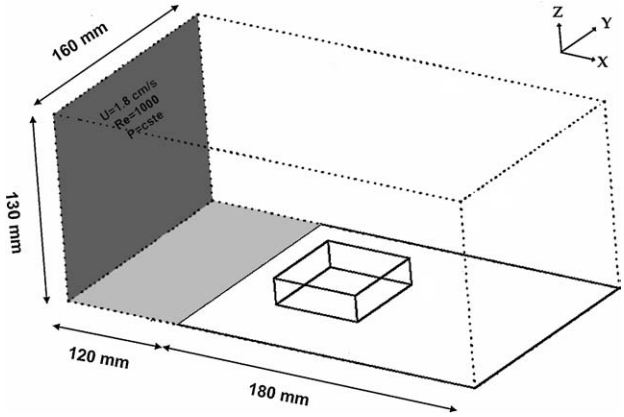

Fig. 4. Calculation domain.

Fig. 4. Domaine de calcul.

direction and is stopped by the external flow at the saddle point B at $0.51D$ from the upstream face of the obstacle. The whole vortical system is then evacuated in the main flow towards the sides of the obstacle.

Above the stagnation point A, the external flow separates from the leading edge of the obstacle (Fig. 3). It generates a low pressure zone, leading to the appearance of arch-shaped vortices which are released periodically in obstacle wake.

3. Calculation tool and numerical parameters

Calculations are carried out with a finite differences 3D direct numerical simulation code. Numerical integration is second order accurate in space (central difference scheme) and second order accurate in time (explicit McCormack scheme). A full description can be found in [9]. Fig. 4 shows the calculation domain. It is a square box of 300 mm $\times$ 160 mm $\times$ 130 mm in the X, Y and Z directions respectively. The obstacle is placed at 40 mm from the leading edge of the plate, on the frontier $Z = 0$ and is centred in Y. Its base is 60 mm by 60 mm and its height H is 18 mm. The leading edge of the plate is at 120 mm from the inlet of the channel. This position allows the

flow to develop with minimal interaction with the upstream boundary. The importance of this region will be discussed later in this Note. The plate covers the rest of the frontier $Z = 0$. The reference frame origin is centred in Y, on the intersection line between the plate surface and the upstream face of the obstacle. The flow under study is basically a channel flow with an obstacle and no slip condition is imposed on plate surface and on the obstacle. A flow of water at $Re = 1000$ (based on the same parameters than for the experiments) is imposed at the inlet of the channel ($X = 0$). The boundary condition for the outlet and sides of the channel is that of an outflow boundary (zero velocity gradient). Various boundary conditions have been tested for the sides of the calculation domain, including a no slip boundary condition and a slipping wall condition. No confinement effect could be observed. The zero velocity gradient condition has been chosen since the dimensions of the calculation domain did not reproduce exactly the dimension of the experimental channel. Concerning the zero velocity gradient condition at the outlet, it is believed that a sufficient distance between the obstacle and the outlet would reduce the influence on the flow near the obstacle and on its upstream sides. This has been confirmed by comparing results obtained with different dimensions of the calculation domain in the streamwise direction. The calculations have been carried out using a Cartesian non-uniform grid containing 250 cells in the X direction, 80 cells in the Y direction and 180 in the Z direction, which gives a total of 3.6 million cells. The grid is uniform in the X and Y directions and includes in the Z direction a refined zone at the vicinity of the plate (0.2 mm/cell) with a progressive increase of the cell size when Z increases (0.5 mm/cell at the top of the obstacle, 1.0 mm/cell at the half height of the channel and 1.2 mm/cell at the top of the channel). Stability is ensured by a CFL criterion (Courant–Friedrichs–Lewy) based on the cells dimensions and the local fluid velocity.

An early comparison between simulations and experiments had been conducted by Calluaud et al. [7] for the same experimental configuration but with no numerical development zone on the upstream part of the flow. Whereas the 4-vortices stationary vortical system had been obtained numerically, several differences between experiments and calculations were found concerning, among other things, the altitude of stagnation point A and the amplitude of the separation zone. This gave a poor description of the temporal evolution of vortex shedding in the obstacle wake. Due to the obstacle and the horseshoe vortex, the influence of the obstacle on the external flow extends far upstream of the leading edge of the plate, which could not be retrieved by the calculations. Therefore, a development zone was added between the leading edge of the plate and the inlet of the domain to avoid the interaction between pressure perturbation due to the obstacle and a the numerical boundary. Several distances were tested. A distance of one obstacle diameter (60 mm) still leads to significant discrepancies, two diameters (120 mm) yields an significant improvement and three diameters (180 mm) gives the same result. A distance larger or equal to 120 mm upstream of the plate is therefore adequate.

4. Comparisons

Simulations with this development zone lead to a significant improvement of the results. As in the previous case, a stationary 4-vortices system is found at the leading edge of the obstacle but with a fairly good agreement as concerns the position of singular points (Fig. 2 and Table 1). Positions of singular points in Table 1 have been extracted from plots similar to Figs. 2(a) and 2(b). Slight discrepancies however remain. Abscissas obtained from calculations are slightly smaller than those given by experiments and vortex 3 is not captured by the calculation. This is believed to be a consequence of the grid size which is too coarse in the streamwise direction in this region. Nevertheless, this vortex is believed to be of no influence on the global structure of the flow and therefore is ignored in the present analysis. The most significant difference concerns the position of the point B (Fig. 2(b)), which shows that the horseshoe vortex obtained numerically expands further upstream as compared with the one observed experimentally.

A difference between experiments and calculations still remains for the vertical component of the velocity profile at the leading edge of the plate (Fig. 5). In the experiments, the upstream flow is strongly influenced by the horseshoe vortex and a stagnation point at the leading edge of the plate.

Table 1
Singular points in the section $Y = 0$. Comparison between simulations and experiments. Numerical 1: case without a development zone. Numerical 2: case with a development zone

Tableau 1
Points singuliers dans la section $Y = 0$. Comparaison simulations/expériences. Simulation 1 : sans zone de développement. Simulation 2 : avec zone de développement

	Experimental		Numerical 1		Numerical 2	
	X/D	Z/H	X/D	Z/H	X/D	Z/H
Centre of vortex 1	−0.114	0.330	−0.093	0.290	−0.132	0.330
Centre of vortex 2	−0.308	0.173	−0.249	0.158	−0.327	0.170
Point A	0	0.790	0	0.633	0	0.786
Point B	−0.509	0	−0.355	0	−0.540	0
Point C	−0.241	0.230	−0.196	0.233	−0.266	0.233

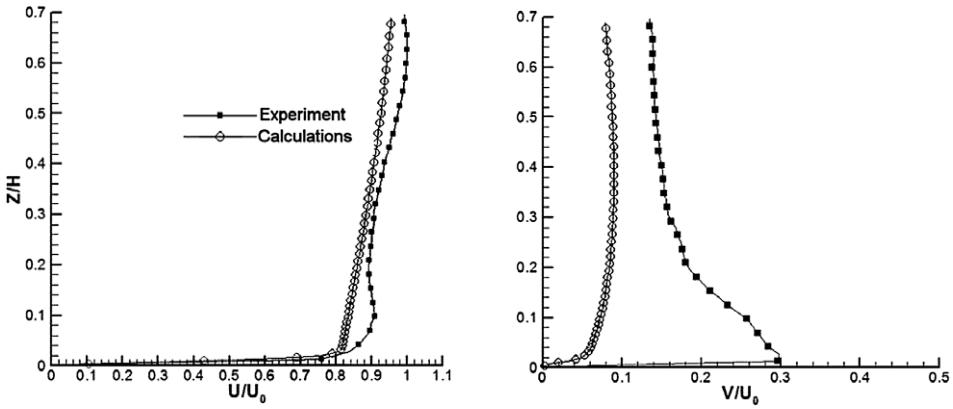

Fig. 5. Experimental and numerical velocity profiles u/U_0 and v/U_0 at the leading edge of the plate for the section $Y/D = 0$.

Fig. 5. Profils de vitesse u/U_0 et v/U_0 numériques et expérimentaux au bord d'attaque de la plaque pour $Y/D = 0$.

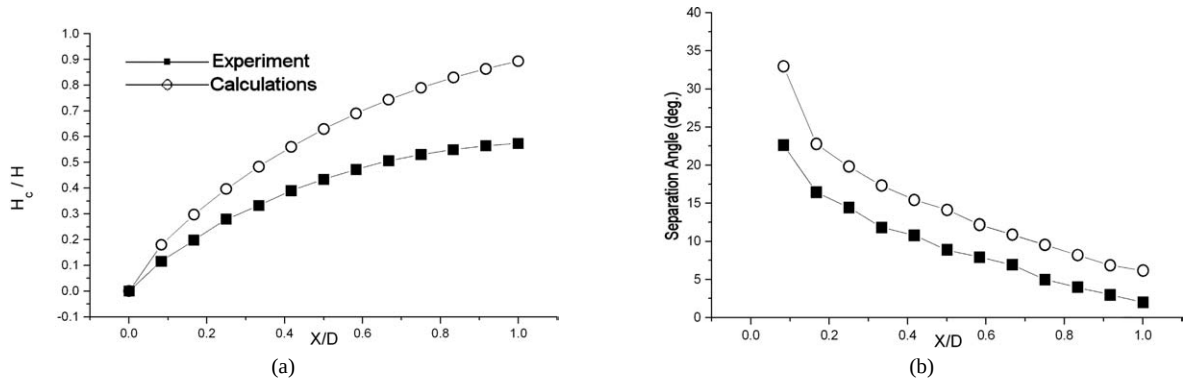

(a) (b)

Fig. 6. Characteristics of the separation zone in the section $Y/D = 0$. (a) Heigh of the separation zone H_c as a function of the position on the streamwise axis X/D. (b) Evolution of the angle of the separation zone as a function of the position on the streamwise axis X/D.

Fig. 6. Caractéristiques de la zone de séparation dans la section $Y/D = 0$. (a) Hauteur de la zone de séparation H_c en fonction de l'abscisse X/D. (b) Evolution de l'angle de la zone de séparation en fonction de l'abscisse X/D.

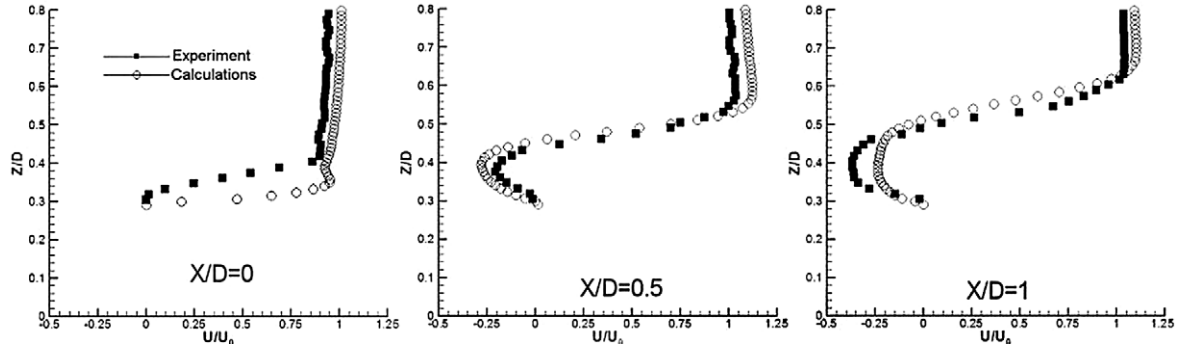

Fig. 7. Component u/U_0 of the mean velocity profile in the section $Y/D = 0$, above the obstacle for various positions X/D.

Fig. 7. Profils de vitesse de la composante moyenne u/U_0 dans la section $Y/D = 0$ pour différentes positions en X/D.

Upstream of the plate, streamlines are significantly deflected vertically. Simulations do not capture this phenomenon due to the upper boundary conditions. This leads to a lower position of the point A in the calculation and the separation of the flow is more pronounced in the simulations than in the experiments (Fig. 6).

The velocity profiles above the obstacle are in good agreement (Fig. 7), demonstrating the improvement given by the addition of the development zone as compared with earlier calculations [7]. The experimental and numerical vortex shedding frequencies only differ by about 10% (0.215 Hz from experiments, 0.238 Hz from calculations) indicating that the dynamics of the wake flow is well reproduced despite the aforementioned discrepancies.

5. Conclusions

The flow around a surface-mounted block for a Reynolds number of 1000 and for a short distance between the leading edge of the plate and the upstream face of the obstacle is investigated in this article. Numerical and experimental evidence indicate that the upstream region of the obstacle, among characteristic values such as boundary layer thickness and nature or blockage ratio, has a strong influence on the structure of the laminar junction flow and therefore should be handled with care in numerical simulations.

It is found important to place the upstream boundary at a sufficient distance from the obstacle to eliminate interactions between the pressure perturbation associated with this object and the boundary. By the introduction of the development zone upstream the plate in the calculation domain, numerical results have been improved. The steady structure at the leading edge of the obstacle that is observed experimentally and composed by four vortices, is well described. The topology of the junction flow is also correctly reproduced, despite a slightly under-predicted position of the separation point at the leading edge of the obstacle.

Experimental results also reveal that due to a combined effect of the horseshoe vortex generated by the junction flow and of the stagnation point at the leading edge of the plate, streamlines are already deflected upstream of the plate. This behaviour cannot be captured by the calculations due to boundary conditions on the development zone and it is believed that this is the source of the remaining discrepancies between experiments and calculations. The separation angle above the obstacle is slightly over predicted by calculations but streamwise velocity profiles still show a good agreement and periodical mechanisms of vortex generation and shedding are globally identical [8].

References

[1] J.C.R. Hunt, C.J. Abell, J.A. Peterka, H. Woo, Kinetical studies of the flows around free or surface-mounted obstacles, applying topology to flow visualization, J. Fluid Mech. 86 (1) (1978) 179–200.

[2] I.P. Castro, A.G. Robins, The flow around a surface-mounted cube in uniform and turbulent streams, J. Fluid Mech. 79 (2) (1977) 307–335.
[3] J.H. Chou, S.Y. Chao, Branching of a horseshoe vortex around surface-mounted rectangular cylinders, Exp. Fluids 28 (2000) 394–402.
[4] C.J. Baker, The laminar horseshoe vortex, J. Fluid Mech. 95 (2) (1979) 347–367.
[5] R.J. Martunizzi, C. Tropea, The flow around surface-mounted obstacles placed in a fully developed channel flow, J. Fluid Engrg. ASME 115 (1993) 85–92.
[6] W. Rodi, J.H. Ferziger, M. Breuer, M. Pourquie, Status of large eddy simulation: results of a workshop, J. Fluid Engrg. ASME 119 (2) (1997) 248–262.
[7] D. Calluaud, L. David, S. Rouvreau, P. Joulain, Ecoulement laminaire autour d'un cylindre de section carrée. Comparaison calcul expérience, in: Congrès Français de Mécanique, Nancy, n^{o} 372, 2001, pp. 1–6.
[8] D. Calluaud, Développement d'une méthode de mesures tridimensionnelles par PIV stéréoscopique. Application à l'étude de l'écoulement naissant et établi autour d'un parallélépipède, Thèse de l'Université de Poitiers, 2003.
[9] K.B. McGrattan, H.R. Baum, R.G. Rehm, A. Hamins, G.P. Forney, J.E. Floyd, Fire Dynamics Simulator – Technical Reference Guide (Version 2), 2000.